ROBUST MINIMUM VOLUME SIMPLEX ANALYSIS FOR HYPERSPECTRAL UNMIXING

Alexander Agathos[(1)], *Jun Li*[(2)], *José M. Bioucas-Dias*[(3)], *Antonio Plaza*[(4)]

[(1)] Computer Science Department, West University of Timisoara, Romania
[(2)] School of Geography and Planning, Sun Yat-Sen University, Guangzhou, P. R. China
[(3)] Instituto de Telecomunicações, Instituto Superior Técnico, Universidade de Lisboa, Portugal
[(4)] Hyperspectral Computing Laboratory, University of Extremadura, Cáceres, Spain

ABSTRACT

Most blind hyperspectral unmixing methods exploit convex geometry properties of hyperspectral data. The *minimum volume simplex analysis* (MVSA) is one of such methods which, as many others, estimates the minimum volume (MV) simplex where the measured vectors live. MVSA was conceived to circumvent the matrix factorization step often implemented by MV based algorithms and also to cope with outliers, which compromise the results produced by MV algorithms. Inspired by the recently proposed *robust minimum volume estimation* (RMVES) algorithm, we herein introduce the robust MVSA (RMVSA), which is a version of MVSA robust to noise. As in RMVES, the robustness is achieved by employing chance constraints, which control the volume of the resulting simplex. RMVSA differs, however, substantially from RMVES in the way optimization is carried out. The effectiveness of RVMSA is illustrated by comparing its performance in simulated data with the state-of-the-art.

Index Terms— Hyperspectral imaging, spectral unmixing, endmember identification, minimum volume simplex analysis (MVSA), chance constraints.

1. INTRODUCTION

Hyperspectral unmixing (HU) aims at estimating the number of reference substances, also called *endmembers*, their spectral signatures, and their *abundance fractions* in hyperspectral imagery [1]. In practice, hyperspectral unmixing is a source separation problem [2]. Compared with the canonical source separation scenario, the sources in hyperspectral unmixing are statistically dependent, and the observed mixture is either linear or nonlinear in nature [3]. The linear mixing model holds when the mixing scale is macroscopic [4, 5].

Linear unmixing techniques can be classified into statistical and geometrical-based [1]. The former category addresses spectral unmixing as an inference problem, often formulated under the Bayesian framework, whereas the latter category exploits the fact that the spectral vectors (under the linear mixing model) are in a simplex whose vertices correspond to the endmembers. The main research lines presented in recent years under this framework belong to two different groups: a) pure pixel based algorithms assume that the scene contains at least one pure pixel per endmember [1]; b) more recently, several algorithms dropped this assumption by assuming that no pure pixels may be present in real hyperspectral scenes [1, 2, 6]. In this case, a widely used strategy is to fit a simplex of minimum volume to the data set. Relevant works exploiting this direction are the minimum volume constrained non-negative matrix factorization (MVC-NMF) [7], the *minimum volume simplex analysis* MVSA [8], the *simplex identification via split augmented Lagrangian* (SISAL) algorithm [9], the minimum-volume enclosing simplex (MVES) [10], the *collaborative nonnegative matrix factorization* [11] (CoNMF), and the RMVES [12], among others (see [1, 2] for an exhaustive account of MV based algorithms).

The MV based approach to HU is quite appealing and underlies a large number of blind HU methods introduced in the last 20 years. The simplex of MV is, however, highly sensitive to noise and outliers, what limits its applicability. Aiming at endowing the MV criterion with robustness to outliers, MVSA [8] replaces the hard abundance non-negativity constraint with a soft abundance non-negativity enforced by the hinge function. This robust to outliers version of MVSA is efficiently implemented by the SISAL [9] algorithm.

In this work, inspired by chance constraints [13] used in the RMVES, we develop a robust to noise version of MVSA (RMVSA). Although RMVSA solves the same problem as RMVES, we adopt a different optimization strategy, which turned out to be effective in terms of computational complexity and of the quality of the estimates.

The remainder of the paper is organized as follows. Section 2 describes the proposed RMVSA algorithm. Section 3 presents experiments with simulated data. A quantitative assessment to other popular endmember identification algorithms is also provided. Section 4 concludes the paper with some remarks and future research lines.

2. ROBUST MINIMUM VOLUME SIMPLEX ANALYSIS (RMVSA)

Let the data spectral vectors $\mathbf{Y} \equiv [\mathbf{y}_1, \ldots, \mathbf{y}_n] \in \mathbb{R}^{p \times n}$ be a matrix holding in its columns spectral vectors $\mathbf{y}_i \in \mathbb{R}^p$, where p is the number of endmembers and n is the number of pixels. We assume that a dimensionality reduction step (see, *e.g.*, [14]) was applied to the data such that the vectors $\mathbf{y}_i \in \mathbb{R}^p$ are the coordinates of the original vectors with respect to a basis of the subspace spanned by the original measured vectors. Under the linear mixing model, we have

$$\begin{aligned} \mathbf{Y} &= \mathbf{MS} + \mathbf{W} \\ \text{s.t.:} &\quad \mathbf{S} \geq 0, \ \mathbf{1}_p^T \mathbf{S} = \mathbf{1}_n^T, \end{aligned} \quad (1)$$

where $\mathbf{M} \equiv [\mathbf{m}_1, \ldots, \mathbf{m}_p] \in \mathbb{R}^{p \times p}$ is the mixing matrix ($\mathbf{m}_i$ denotes the i-th endmember signature and p is the number of endmembers), and $\mathbf{S} \in \mathbb{R}^{p \times n}$ is is the abundance matrix containing the fractions of each endmember, $\mathbf{1}_m = [1, 1, \ldots, 1]^T$ is a $m \times 1$ vector of ones, $\mathbf{W} \equiv [\mathbf{w}_1 \ldots, \mathbf{w}_N]$ accounts for noise, and the notation $(\cdot)^T$ stands for vector or matrix transpose. Owing to physical constraints [15], for each pixel, the fraction vectors should be no less than zero, and sum to 1. Therefore, the spectral vectors $\mathbf{y}_i$, belong to a simplex set with vertices $\mathbf{m}_i$. MVSA aims at finding the matrix $\mathbf{M}$ with minimum volume defined by its columns under the constraints in (1). As shown in [8], an equivalent formulation of this criterion in the absence of noise is as the follows:

$$\begin{aligned} \widehat{\mathbf{Q}} &= \arg \max_{\mathbf{Q}} \ \log |\det(\mathbf{Q})| \\ \text{s.t.:} &\quad \mathbf{QY} \geq 0, \ \mathbf{1}_p^T \mathbf{Q} = \mathbf{a}, \end{aligned} \quad (2)$$

where $\mathbf{Q} \equiv \mathbf{M}^{-1}$ and $\mathbf{a} = \mathbf{1}_n^T \mathbf{Y}^T (\mathbf{YY}^T)^{-1}$.

MVSA solves problem (2) using sequential quadratic programming (SQP). In addition to the criterion (2), a robust to outliers version called SISAL [9] was also introduced. In this robust version, the constraint $\mathbf{QY} \geq 0$ is replaced with a soft constraint $-\mathbf{1}^T \text{hinge}(-\mathbf{QY})\mathbf{1}$, where $\text{hinge}(\mathbf{x})$ is an element-wise operator that, for each component, yields the negative part of $\mathbf{x}$.

From (1) we have $\mathbf{QY} = \mathbf{S} + \mathbf{QW}$. When the noise is not negligible, the constraint $\mathbf{QY} \geq 0$ act on $\mathbf{S} + \mathbf{QW}$ and not only on $\mathbf{S}$, inflating the estimated simplex with respect to the true one. To mitigate this negative effect, and inspired by the RMVES method [12], we replace the constraint $\mathbf{QY} \geq 0$ with the probability constraints $P([\mathbf{QY} - \mathbf{QW}]_{in} \geq 0) \geq \eta$, for $i = 1, \ldots, p$ and $n = 1, \ldots, N$, where $P(\cdot)$ denotes probability and $[\mathbf{X}]_{ij}$ is the (i, j) component of matrix $\mathbf{X}$.

Let $\mathbf{q}_i$ denote the column vector formed by the ith row of $\mathbf{Q}$ and assume that the noise random vectors $\mathbf{w}_i$, for $i = 1, \ldots, N$, are Gaussian distributed with zero mean and projected covariance matrix $\mathbf{D}_w$, where $\mathbf{D}_w = \mathbf{U}_p^T \mathbf{D} \mathbf{U}_p$. $\mathbf{D}$ is the noise covariance matrix and $\mathbf{U}_p$ is the affine projection matrix to $\mathbb{R}^p$. With this definition in place, we reformulate the unmixing problem using probability constraints as follows:

$$\begin{aligned} \widehat{\mathbf{Q}} &= \arg \min_{\mathbf{Q}} \ -\log |\det(\mathbf{Q})| \\ \text{s.t.:} &\quad \mathbf{q}_i^T \mathbf{y}_n \geq \Phi^{-1}(\eta) \sqrt{\mathbf{q}_i^T \mathbf{D}_w \mathbf{q}_i}, \\ &\quad \mathbf{1}_p^T \mathbf{Q} = \mathbf{a}, \forall i \in \{1, \cdots, p\}, \forall n \in \{1, \cdots, N\}, \end{aligned} \quad (3)$$

where $\Phi(\cdot)$ denotes the cumulative distribution function of the standard normal random variable (Gaussian random variable with zero mean and unit variance).

From (3), it can be inferred that, when $\eta = 0.5$, $\Phi^{-1}(\eta) = 0$ and (3) is equivalent to MVSA under hard constraints. When $\eta < 0.5$, $\Phi^{-1}(\eta) < 0$, the terms $\mathbf{q}_i \mathbf{y}_n$ may take negative values meaning that the RMVSA solution approaches the real simplex. This scenario is illustrated in Fig. 1.

The optimization problem (3) is difficult since the objective function is nonconvex and the constraints are nonlinear and, if $\eta < 0.5$, nonconvex. In this work, we propose a relaxation of the inequality constraint which can be defined as follows. At the $t + 1$ iteration, we have

$$\begin{aligned} \mathbf{Q}^{(t+1)} &= \arg \min_{\mathbf{Q}} \ -\log |\det(\mathbf{Q})| \\ \text{s.t.:} &\quad \mathbf{q}_i^T \mathbf{y}_n \geq \Phi^{-1}(\eta) \sqrt{\mathbf{q}_i^{(t)T} \mathbf{D}_w \mathbf{q}_i^{(t)}}, \\ &\quad \mathbf{1}_p^T \mathbf{Q} = \mathbf{a}, \\ &\quad \forall i \in \{1, \cdots, p\}, \forall n \in \{1, \cdots, N\}, \end{aligned} \quad (4)$$

where $\mathbf{q}_i^{(t)}$ is the ith row of $\mathbf{Q}^{(t+1)}$. The advantage of (4) is that the constraints are linear and, thus, we may still apply the SQP based approach used in the original MVSA [8]. In the following we will briefly describe the MVSA algorithm [8] and its modification aimed at solving the optimization (4).

Denote $\mathbf{q} \equiv \text{vec}(\mathbf{Q})$, i.e., the columnwise stacking of the columns of $\mathbf{Q}$ and define $f(\mathbf{q}) \equiv -\log |\det(\mathbf{Q})|$. We adopt the majorization minimization strategy to solve (4), which amounts to iteratively minimize a majorizer of f, denoted as $\phi(\mathbf{q}; \mathbf{q}^{(t)})$, such that $\phi(\mathbf{q}^{(t)}; \mathbf{q}^{(t)}) = f(\mathbf{q}^{(t)})$, $\phi(\mathbf{q}; \mathbf{q}^{(t)}) \geq f(\mathbf{q}^{(t)})$, and $\phi(\mathbf{q}, \mathbf{q}^{(t)})$ is easy to minimize. Using the fact that the gradient and the Hessian of f are, respectively, given by $\mathbf{g}(\mathbf{q}) = \text{vec}(-\mathbf{Q}^{-T})$ and $\mathbf{H}(\mathbf{q}) = \mathbf{K}_n[\mathbf{Q}^{-T} \otimes \mathbf{Q}^{-1}]$, where $\mathbf{K}_n$ is the comutation matrix (*i.e.*, $\mathbf{K}_n \text{vec}(\mathbf{A}) = \text{vec}(\mathbf{A}^T)$) (see [9] for details), we define the following local majorizer for f:

$$\phi(\mathbf{q}; \mathbf{q}^{(t)}) \equiv \beta^{(t)} + \mathbf{c}^{(t)T} \mathbf{q} + \frac{1}{2} \mathbf{q}^T \mathbf{G}^{(t)} \mathbf{q} \quad (5)$$

where $\mathbf{c}^{(t)} = \mathbf{g}(\mathbf{q}^{(t)}) - \mathbf{H}(\mathbf{q}^{(t)}) \mathbf{q}^{(t)}$ and $\mathbf{G}^{(t)} = \text{diag} \mathbf{H}(\mathbf{q}^{(t)})$.

Define $\mathbf{A}_I = \mathbf{Y}^T \otimes \mathbf{I}_p$, $\mathbf{A}_E = \mathbf{I}_p \otimes \mathbf{1}_p$, $\mathbf{b}_I^{(t)} = \text{vec}([\Phi^{-1}(\eta) \sqrt{\mathbf{q}_i^{(t)T} \mathbf{D}_w \mathbf{q}_i^{(t)}}, i = 1, \ldots, p]^T \otimes \mathbf{1}_N^T)$ and $\mathbf{b}_E = \mathbf{a}$, where $\otimes$ is the Kroneker product and $\mathbf{I}_p$ is the identity matrix. Therefore, the minimization of (5) subject to the constrains shown in (4) may be written compactly as

$$\begin{aligned} \min \ \phi(\mathbf{q}; \mathbf{q}^{(t)}) &= \mathbf{c}^{(t)T} \mathbf{q} + \frac{1}{2} \mathbf{q}^T \mathbf{G}^{(t)} \mathbf{q} \quad (6) \\ \text{s.t.:} &\quad \mathbf{A}_I \mathbf{q} \geq \mathbf{b}_I^{(t)}, \ \mathbf{A}_E \mathbf{q} = \mathbf{b}_E, \end{aligned}$$

which is a quadratic programming (QP) problem. Algorithm 1 shows the proposed SQP RMVSA algorithm.

Algorithm 1 RMVSA pseudocode

1: **INPUT:** $\mathbf{A}_I$, $\mathbf{A}_E$, $\mathbf{b}_E$, $\mathbf{q}_0$, where $\mathbf{q}_0$ an initial solution
2: **COMMENT:** $f(\mathbf{q}) = -\log|\det(\mathbf{Q})|$ is the objective function
3: $Convergence \leftarrow false, Iterations \leftarrow 0, \mathbf{q} = \mathbf{q}_0$
4: **repeat**
5:     Compute $\mathbf{c}$, $\mathbf{G}$, and $\mathbf{b}_I$ ($defined\ after$ (5))
6:     $\mathbf{q} \leftarrow$ solution of the quadratic optimization (6)
7:     **if** $f(\mathbf{q}_0) < f(\mathbf{q})$ **then**
8:         do line search until $f(\mathbf{q}_0) > f(\mathbf{q})$
9:         **//Take the middle of $\mathbf{q}_0$, $\mathbf{q}$**
10:     **end if**
11:     **if** $|f(\mathbf{q}_0) - f(\mathbf{q})| < threshold$ **then**
12:         $Convergence \leftarrow true$
13:     **end if**
14:     $\mathbf{q}_0 \leftarrow \mathbf{q}$
15:     $Iterations \leftarrow Iterations + 1$
16: **until** $Convergence$ **or** $Iterations \geq 4$

As discussed in [1], a major issue for a MV algorithm is that it is not strictly convex or concave, thus a proper initialization is very important. In this work, we use the MVSA solution as an initialization for RMVSA. MVSA can be executed by the same algorithm by setting $\mathbf{b}_I = \mathbf{0}$. Another important issue for Algorithm 1 is its convergence. Although we still do not have a proof convergence, we have systematically observed that a maximum of 4 iterations were sufficient for RMVSA to converge.
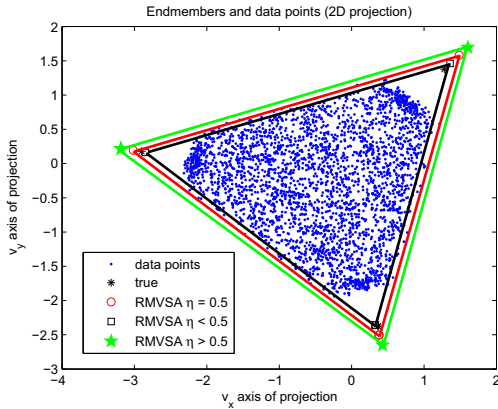

Fig. 1. Plot of the endmember simplex for $\eta < 0.5$, $\eta = 0.5$ and $\eta > 0.5$

3. EXPERIMENTS

In this section we compare the RMVSA algorithm presented in this work with other state of the art algorithms for end-member extraction, specifically RMVES [12], MVSA [8], MVES [10] and N-FINDR [16]. For a given data set, all algorithms were run just once whereas, owing to its sensitivity to the initialization, RMVES was run 10 times with $\mathbf{\Phi}^{-1}(\eta) = -0.3$ taking the best result as explicitly suggested by its Authors. To evaluate the performance of the different algorithms, the estimated abundance fractions ($\widehat{\mathbf{A}}$) generated by inverse constrained minimization, and the signature estimates ($\widehat{\mathbf{M}}$) are compared with the true ones ($\mathbf{A}$ and $\mathbf{M}$, respectively). Both $\mathbf{A}$ and $\widehat{\mathbf{A}}$ are acquired by the inverse minimization process using $\mathbf{M}$ and $\widehat{\mathbf{M}}$ respectively. We use several metrics to evaluate the proposed approach. The first one is the mean square error (MSE), denoted as $\| \epsilon \|_F = \| \widehat{\mathbf{M}} - \mathbf{M} \|_F$ where $\| \cdot \|_F$ stands for the Frobenius norm. Another metric considered in our experiments is the reconstruction error, computed as $r\epsilon = \| \widehat{\mathbf{Y}} - \mathbf{Y} \|_F = \| \widehat{\mathbf{M}}\widehat{\mathbf{A}} - \mathbf{Y} \|_F$. The third metric used in this work is the spectral angle distance (SAD) (in degrees) expressed as $\text{SAD} = \cos^{-1}(\frac{\mathbf{m}_i^T \widehat{\mathbf{m}}_i}{\|\mathbf{m}_i\|\|\widehat{\mathbf{m}}_i\|})$ [3]. All algorithms have been implemented in Matlab.

Our experiments have been conducted on a synthetic image of size 100×100 pixels and 200 bands. The spectral signatures are random uniform and selected from the USGS library [17] and are used to construct the data-sets under the linear mixture model (1). The data are Dirichlet distributed and uniformly distributed over the simplex. Zero-mean white Gaussian noise, defined as $\text{SNR} = 10 \log_{10} (\mathbb{E}[\|\mathbf{Y}\|_F^2]/\mathbb{E}[\|\mathbf{W}\|_F^2])$ (dB), has been added to the synthetic scene. We distinguish two cases, first when pure pixels exist, second when non pure pixels exist in the synthetic image.

3.1. Pure pixel based experiments

In the first experiment, we evaluate the proposed RMVSA algorithm by assuming that pure pixels are present in the considered data set, simulated with $p = 5$ endmembers. Tables 1 and 2 show the results obtained by the aforementioned methods for the considered scene with different noise levels. It can be observed that both RMVSA and RMVES perform better than their corresponding hard constrained versions of MVSA and RMVES, respectively. RMVSA performs slightly better than RMVES due to the fine tuning of the probability parameter. Both RMVES and RMVSA manage to achieve similar results as N-FINDR which is not the case for MVSA and MVES which is their major weakness.

3.2. Non pure pixel based experiments

In this subsection, we evaluate RMVSA by assuming that no pure pixels exist in the considered image (the maximum purity is 0.8). The same experimental set was constructed as with the previously experiment. Tables 3 and 4 show the obtained results from the same methods for the considered

Table 1. Comparison of endmember extraction algorithms on a synthetic image containing pure mineral signatures from the USGS library under different noise levels.

dB	RMVSA				RMVES			MVSA			MVES			N-FINDR		
	$\lVert \epsilon \rVert_F$	$r\epsilon$	SAD	$\lvert\Phi^{-1}(\eta)\rvert$	$\lVert \epsilon \rVert_F$	$r\epsilon$	SAD	$\lVert \epsilon \rVert_F$	$r\epsilon$	SAD	$\lVert \epsilon \rVert_F$	$r\epsilon$	SAD	$\lVert \epsilon \rVert_F$	$r\epsilon$	SAD
40	0.004	6.4e-6	0.2	0.05	0.13	4.3e-5	0.6	0.007	6.4e-6	0.4	0.009	6.4e-6	0.5	0.002	7.8e-6	0.6
30	0.01	2e-5	0.5	0.07	0.04	3.7e-5	2.1	0.02	2e-5	1.3	0.13	2e-5	3.5	0.003	2.5e-5	1.9
20	0.02	6.5e-5	1.3	0.08	0.03	6.8e-5	2.2	0.12	6.5e-5	5.1	0.12	6.5e-5	5	0.01	8.3e-5	6.3
10	0.06	2.1e-04	3	0.1	0.07	2.1e-04	3.3	0.99	2.1e-4	18.8	0.94	2.1e-4	18.1	0.04	2.5e-04	18.3

Table 2. Comparison of endmember extraction algorithms on a synthetic image containing random, uniformly distributed, pure pixels under different noise levels.

dB	RMVSA				RMVES			MVSA			MVES			N-FINDR		
	$\lVert \epsilon \rVert_F$	$r\epsilon$	SAD	$\lvert\Phi^{-1}(\eta)\rvert$	$\lVert \epsilon \rVert_F$	$r\epsilon$	SAD	$\lVert \epsilon \rVert_F$	$r\epsilon$	SAD	$\lVert \epsilon \rVert_F$	$r\epsilon$	SAD	$\lVert \epsilon \rVert_F$	$r\epsilon$	SAD
40	0.001	8.9e-6	0.1	0.02	0.004	9e-6	0.23	0.004	8.9e-6	0.22	0.006	8.9e-6	0.3	0.001	1.1e-5	0.5
30	0.006	2.8e-5	0.3	0.03	0.018	3.45e-5	0.7	0.02	2.8e-5	0.8	0.13	2.8e-5	3	0.005	3.4e-5	1.6
20	0.02	8.8e-5	1	0.04	0.03	8.8e-5	1.4	0.06	8.8e-5	3	0.07	8.8e-5	3.3	0.02	1.1e-4	5.1
10	0.04	2.7e-4	2	0.04	0.06	2.8e-4	3	0.21	2.7e-4	9.8	0.24	2.8e-4	10.7	0.04	3.3e-4	15.6

scenes with different noise levels. As expected, the algorithms without the pure pixel assumption such as RMVSA, RMVES, MVSA and MVES outperform the pure pixel-based N-FINDR algorithm. It can also be observed that RMVSA performs slightly better than RMVES for all noise levels.

3.3. Computational complexity

In this subsection we present the processing times of RMVSA (including initialization), RMVES, MVSA, MVES on a synthetic image of 100×100 image with SNR = 30dB for different number of end-members. The times (in secs) were measured in a 4-core desktop PC at 3.0 GHz and 8 GB of RAM. In Table 5 it can be observed that RMVSA takes twice the time of MVSA and takes significant less time than RMVES.

Table 5. Processing time (seconds) obtained on a synthetic image for different number of endmembers.

p	RMVSA	RMVES	MVSA	MVES
5	4.1	29.7	2.4	15.3
10	42.9	1788	22.9	546

4. CONCLUSIONS AND FUTURE LINES

In this work, we have introduced a new robust minimum volume simplex analysis (RMVSA) algorithm for HU. By including chance constraints, the proposed RMVSA is able to deal with scenarios in which noise exist. An important contribution of this work is the relaxation of the chance constraint, such that the constraints of the optimization problem are linear. This brings great advantages from both the theoretical

and computational viewpoints. The proposed RMVSA algorithm was evaluated using different simulated hyperspectral data sets, in comparison with other state of the art minimum volume based algorithms. The experimental results showed that the proposed algorithm is very efficient for unmixing highly mixed and noisy data. Future work will focus on evaluating the proposed methodology using real data and on providing theoretical values for the η parameter based on the distribution of the data. We will also search for a theoretical upper bound for the number of iterations needed for convergence of the proposed optimization.

Acknowledgement

REFERENCES

[1] J. Bioucas-Dias, A. Plaza, N. Dobigeon, M. Parente, Q. Du, P. Gader, and J. Chanussot, "Hyperspectral unmixing overview: Geometrical, statistical, and sparse regression-based approaches," *IEEE J. Sel. Topics Appl. Earth Observ. and Remote Sens.*, vol. 5, no. 2, pp. 354–379, 2012.

[2] W.-K. Ma, J. Bioucas-Dias, T.-H. Chan, N. Gillis, P. Gader, A. Plaza, A. Ambikapathi, and C.-Y. Chi, "A signal processing perspective on hyperspectral unmixing: Insights from remote sensing," *Signal Processing Magazine, IEEE*, vol. 31, no. 1, pp. 67–81, Jan 2014.

[3] N. Keshava and J. F. Mustard, "Spectral unmixing,"

Table 3. Comparison of endmember extraction algorithms on a synthetic image containing non pure mineral signatures from the USGS library under different noise levels.

dB	RMVSA				RMVES			MVSA			MVES			N-FINDR		
	$\|\epsilon\|_F$	$r\epsilon$	SAD	$\|\Phi^{-1}(\eta)\|$	$\|\epsilon\|_F$	$r\epsilon$	SAD	$\|\epsilon\|_F$	$r\epsilon$	SAD	$\|\epsilon\|_F$	$r\epsilon$	SAD	$\|\epsilon\|_F$	$r\epsilon$	SAD
40	0.004	6.5e-6	0.2	0.05	0.009	6.5e-6	0.4	0.008	6.5e-6	0.02	0.02	6.5e-5	0.5	0.16	8.8e-5	8.5
30	0.01	2.1e-5	0.8	0.07	0.02	2.1e-5	0.7	0.03	2.1e-5	1.6	0.03	2.1e-5	1.6	0.15	8.7e-5	8.3
20	0.03	6.5e-5	1.7	0.08	0.05	6.5e-5	2	0.1	6.5e-5	5.9	0.12	6.5e-5	5.7	0.16	1.1e-4	9.5
10	0.05	2.1e-4	2.4	0.09	0.11	2.1e-4	3.8	0.9	2.1e-4	16.4	0.9	2.1e-4	16.7	0.17	2.7e-04	19.8

Table 4. Comparison of endmember extraction algorithms on a synthetic image containing random, uniformly distributed, non pure pixels under different noise levels.

dB	RMVSA				RMVES			MVSA			MVES			N-FINDR		
	$\|\epsilon\|_F$	$r\epsilon$	SAD	$\|\Phi^{-1}(\eta)\|$	$\|\epsilon\|_F$	$r\epsilon$	SAD	$\|\epsilon\|_F$	$r\epsilon$	SAD	$\|\epsilon\|_F$	$r\epsilon$	SAD	$\|\epsilon\|_F$	$r\epsilon$	SAD
40	0.001	8.7e-6	0.08	0.02	0.005	8.7e-6	0.25	0.003	8.7e-6	0.15	0.003	8.7e-6	0.16	0.12	6.6e-5	6.4
30	0.006	2.8e-5	0.34	0.03	0.01	2.8e-5	0.6	0.02	2.8e-5	0.8	0.02	2.8e-5	1	0.12	8.2e-5	6.8
20	0.01	8.9e-5	0.8	0.04	0.02	8.9e-5	1.1	0.06	8.9e-5	3	0.08	8.9e-5	3.7	0.11	1.2e-4	8
10	0.03	2.7e-4	2	0.04	0.06	2.7e-4	3	0.2	2.7e-4	9.6	0.2	2.7e-4	9.8	0.09	3.4e-4	18

IEEE Signal Processing Magazine, vol. 19, no. 1, pp. 44–57, 2002.

[4] M. Petrou and P. G. Foschi, "Confidence in linear spectral unmixing of single pixels," *IEEE Trans. Geosci. and Remote Sens.*, vol. 37, pp. 624–626, 1999.

[5] J. Settle, "On the effect of variable endmember spectra in the linear mixture model," *IEEE Transactions on Geoscience and Remote Sensing*, vol. 44, pp. 389–396, 2006.

[6] M. Parente and A. Plaza, "Survey of geometric and statistical unmixing algorithms for hyperspectral images," in *Proc. IEEE GRSS Workshop Hyperspectral Image SIgnal Process.: Evolution in Remote Sens. (WHISPERS)*, 2010, pp. 1–4.

[7] L. Miao and H. Qi, "Endmember extraction from highly mixed data using minimum volume constrained nonnegative matrix factorization," *IEEE Transactions on Geoscience and Remote Sensing*, vol. 45, no. 3, pp. 765–777, 2007.

[8] J. Li and J. Bioucas-Dias, "Minimum volume simplex analysis: a fast algorithm to unmix hyperspectral data," *Proc. IEEE International Geoscience and Remote sensing Symposium*, vol. 3, pp. 250–253, 2008.

[9] J. Bioucas-Dias, "A variable splitting augmented lagragian approach to linear spectral unmixing," in *Proc. IEEE GRSS Workshop Hyperspectral Image SIgnal Process.: Evolution in Remote Sens. (WHISPERS)*, 2009, pp. 1–4.

[10] T.-H. Chan, C.-Y. Chi, Y.-M. Huang, and W.-K. Ma, "Convex analysis based minimum-volume enclosing simplex algorithm for hyperspectral unmixing," in *Proc. IEEE international conference on Acoustics, Speech and Signal Processing*, 2009, pp. 1089–1092.

[11] J. Li, J. Bioucas-Dias, and A. Plaza, "Collaborative nonnegative matrix factorization for remotely sensed hyperspectral unmixing," in *Submitted to IEEE Geoscience and Remote Sensing Symposium (IGARSS'12)*, 2012.

[12] A. Ambikapathi, T.-H. Chan, W.-K. Ma, and C.-Y. Chi, "Chance-constrained robust minimum-volume enclosing simplex algorithm for hyperspectral unmixing," *IEEE Transactions on Geoscience and Remote Sensing*, vol. 49, no. 11, pp. 4194–4209, Nov 2011.

[13] S. Boyd and L. Vandenberghe, *Convex Optimization*. Cambridge University Press, 2004.

[14] J. Bioucas-Dias and J. Nascimento, "Hyperspectral subspace identification," *IEEE Trans. Geosci. and Remote Sens.*, vol. 46, no. 8, pp. 2435–2445, 2008.

[15] D. Manolakis, C. Siracusa, and G. Shaw, "Hyperspectral subpixel target detection using linear mixing model," *IEEE Trans. Geosci. Remote Sens.*, vol. 39, no. 7, p. 13921709, 2001.

[16] M. E. Winter, "N-FINDR: an algorithm for fast autonomous spectral end-member determination in hyperspectral data," *Proc. SPIE Image Spectrometry V*, vol. 3753, pp. 266–277, 2003.

[17] R. N. Clark, G. A. Swayze, R. Wise, E. Livo, T. Hoefen, R. Kokaly, and S. Sutley, "Usgs digital spectral library splib06a," *U.S. Geological Survey, Digital Data Series 231*, vol. 1, 2007.